Modelling Simul. Mater. Sci. Eng. 2 (1994) 1111–1121. Printed in the UK

Discretized path integral molecular dynamics with a non-local pseudopotential: simulation of the 3s and 3p states in the sodium atom

G E Jabbour and P A Deymier

Department of Materials Science and Engineering, University of Arizona, Tucson, AZ 85721, USA

Received 14 March 1994, accepted for publication 18 May 1994

Abstract. An expression for the path integral of a single quantum particle in a non-local pseudopotential is derived. This expression is then used to model the behavior of an electron in the potential field of a sodium ion. The amplitude of the 3s and the 3p orbitals of sodium are calculated with an open boundary molecular dynamics simulation. These amplitudes agree favorably with those obtained using the coreless Hartree–Fock approach.

1. Introduction

In recent years the path integral method (PIM) of simulating quantum systems has found extensive use. With the discretized version of the path integral (PI) it is now possible to calculate quantum statistical properties using purely classical statistical techniques. This is usually known as classical isomorphism and is discussed in detail by Chandler and Wolynes [1]. In the isomorphism, a quantum particle is described by a closed chain consisting of beads coupled to each other through harmonic springs. In this case, we can use the classical partition function of the beads to find thermal averages of the quantum particle system.

The most prominent computer simulation techniques that implement the PI are Monte Carlo and molecular dynamics. With these techniques, researchers have been able to investigate a variety of quantum systems ranging from a single quantum particle to many-particle systems. For example, the solvation of an electron in a molten salt [2], in water [3], and in ammonia [4] has been investigated using the PIM. The behavior of fermionic [5] and bosonic [6] many-body systems have also been studied with this method. The PIM may also be used to study the diffusion of hydrogen in metals [7]. Some of the most recent studies based on the PIM involve the electronic structure of Na_3^+ and Na_3 clusters at finite temperature [8], and four electrons in a cavity [9]. The effects of particle exchange were recently incorporated in the path integral [10]. Exchange was also considered in simulating two electrons solvated in a molten salt at high temperature [11]. Particle exchange was implemented in the Fourier path integral technique to study atomic clusters of interacting spinless bosons, and non-interacting identical particles under the influence of harmonic potentials [12].

When performing a simulation one would like to reduce the computational time without loss of accuracy. For example, when performing a calculation of an electronic property of a solid it is easier to simply consider only the valence electrons in the simulation rather than all of the electrons. But in so doing, one must not ignore the effects of the core

0965-0393/94/061111+11$19.50 © 1994 IOP Publishing Ltd

on the valence electrons. The interactions between the core and the valence electrons are incorporated in what is called the pseudopotential. These interactions are usually non-local. The non-locality in the pseudopotential is necessitated by the fact that for most elements, the valence electrons are in different angular momentum states.

Non-local pseudopotentials have been used in quantum Monte Carlo [13] and in diffusion Monte Carlo [14] techniques. They have also been used in quantum molecular dynamics approaches based on the density functional theory [15]. To the best of our knowledge, however, no quantum molecular dynamics path integral (MDPI) simulation has been done that implements a non-local pseudopotential. In this paper, we present an MDPI study of the 3s and the 3p (excited) states in the potential field of a sodium ion. To avoid the problems that arise when using a non-local pseudopotential, mainly the 'fermion disease' arising from the positive parts of the pseudopotential, we report an approximate effective potential that allows the simulation of a quantum particle in a non-local pseudopotential. In section 2 we show how to implement a non-local pseudopotential in the path integral using polar coordinates. The pseudopotentials used in this paper are based on the work done by Bachelet, Hamann, and Schlüter (BHS) [16]. These non-singular pseudopotentials are derived from first principles.

In section 3 the application and results of our study of the 3s and 3p electronic amplitudes in Na are presented. These results are then compared with the coreless Hartree–Fock (CHF) potential method used by Melius and Goddard [17]. The paper ends with a brief discussion of the benefits of using this form of MDPI along with a description of current work and the extendibility of our scheme.

2. Propagator with non-local pseudopotential in polar coordinates

The expression for the PI in polar coordinates has already been derived [18–20]. However, the potential that was used in these derivations was of a local nature. But electrons with different angular momentum states feel a different potential. In this case a non-local pseudopotential must be used to achieve accurate results. We present here a method for incorporating a non-local pseudopotential into the derivation of the PI expression for a single electron.

For a particle moving in a central potential the representation of the propagator, K, based on a Lagrangian formulation of the PI is given by [18–20]

$$K(r_2, r_1, \tau) = \langle r_2|e^{-iH_{op}\tau/\hbar}|r_1\rangle = \sum_{l=0}^{\infty}\sum_{m=-l}^{l} K_l(r_2, r_1, \tau)Y_{lm}^*(\theta_2, \phi_2)Y_{lm}(\theta_1, \phi_1) \tag{1}$$

where τ is the time it takes the particle to move from the initial position r_1 to the final position r_2. The expression $\exp(-iH_{op}\tau/\hbar)$ is the time evolution operator of the quantum particle, and H_{op} is the Hamiltonian operator. The * in equation (1) denotes the complex conjugate.

The amplitude in the radial direction takes the following form [20]:

$$K_l(r_2, r_1, \tau) = \lim_{N\to\infty}(4\pi)^N\left(\frac{m}{2\pi i\epsilon_0}\right)^{3N/2}\int\prod_{i=1}^{N}[R_l(r_i, r_{i-1})]\prod_{i=1}^{N-1} r_i^2\,dr_i \tag{2}$$

where $R_l(r_i, r_{i-1})$ is given by

$$R_l(r_i, r_{i-1}) = [i\pi\epsilon_0/2mr_ir_{i-1}]^{1/2}\exp[(im/2\epsilon_0)(r_i^2 + r_{i-1}^2) - i\epsilon_0 V(r_i)]I_{l+1/2}((m/i\epsilon_0)r_ir_{i-1}). \tag{3}$$

In equation (3), V is the central force potential, ϵ_0 is τ/N, and $I_{l+1/2}(mr_i r_{i-1}/i\epsilon_0)$ is the modified Bessel function.

The quantum statistical partition function for a single electron may be written as

$$Q = \int \mathrm{d}\boldsymbol{r}_1 \langle \boldsymbol{r}_1 | \mathrm{e}^{-\beta H_{\mathrm{op}}} | \boldsymbol{r}_1 \rangle \approx \lim_{P\to\infty} \int \mathrm{d}\boldsymbol{r}_1 \langle \boldsymbol{r}_1 | (\mathrm{e}^{-\beta H_{\mathrm{op}}/P})^P | \boldsymbol{r}_1 \rangle \tag{4}$$

where H_{op} is the Hamiltonian operator for our system and is a sum of the kinetic, local pseudopotential, and non-local pseudopotential operators. By substituting $\tau = -i\hbar\beta$ in equation (4), one can think of the Boltzmann factor, $\exp(-\beta H_{\mathrm{op}})$, as the time evolution operator of the classical particle in imaginary time space.

Upon introducing $(P-1)$ intermediate states in Q we will obtain the PI representation of the partition function

$$Q \approx \int \mathrm{d}\boldsymbol{r}_1\, \mathrm{d}\boldsymbol{r}_2 \ldots \mathrm{d}\boldsymbol{r}_P \langle \boldsymbol{r}_1 | \mathrm{e}^{-\epsilon H_{\mathrm{op}}} | \boldsymbol{r}_2 \rangle \langle \boldsymbol{r}_2 | \mathrm{e}^{-\epsilon H_{\mathrm{op}}} | \boldsymbol{r}_3 \rangle \ldots \langle \boldsymbol{r}_P | \mathrm{e}^{-\epsilon H_{\mathrm{op}}} | \boldsymbol{r}_1 \rangle \tag{5}$$

where $\epsilon = \beta/P$.

Equation (5) carries an interesting picture. The first term represents the path from $\boldsymbol{r}_1$ to $\boldsymbol{r}_2$, the second connects $\boldsymbol{r}_2$ to $\boldsymbol{r}_3$, and so on. Notice that the last term in this equation connects $\boldsymbol{r}_P$ to $\boldsymbol{r}_1$, thus closing the overall path. In other words, the one-electron system is now transformed to look like a polymeric necklace consisting of P beads [1].

With the periodic boundary condition (cyclic condition)

$$\boldsymbol{r}_{P+1} = \boldsymbol{r}_1 \tag{6}$$

we can write the partition function in a more compact form

$$Q \approx \int \prod_{n=1}^{P} \mathrm{d}\boldsymbol{r}_n \langle \boldsymbol{r}_n | \mathrm{e}^{-\epsilon H_{\mathrm{op}}} | \boldsymbol{r}_{n+1} \rangle. \tag{7}$$

Using the Trotter formula, the propagator could be approximated as follows:

$$K(\boldsymbol{r}_{n+1}, \boldsymbol{r}_n, \tau) = \langle \boldsymbol{r}_n | \mathrm{e}^{-\epsilon H_{\mathrm{op}}} | \boldsymbol{r}_{n+1} \rangle \approx \langle \boldsymbol{r}_n | \mathrm{e}^{-\epsilon T_{\mathrm{op}}} \mathrm{e}^{-\epsilon V_{\mathrm{loc}}} \mathrm{e}^{-\epsilon V_{\mathrm{NL}}} | \boldsymbol{r}_{n+1} \rangle \tag{8}$$

where T_{op} is the kinetic energy operator, V_{loc} is the local potential operator, and V_{NL} is the non-local pseudopotential operator.

The non-local pseudopotential operator, in the state representation, that we use in our derivation is of the form [21, 22]

$$V_{\mathrm{NL}} = \sum_{l=0}^{\infty} \sum_{m=-l}^{l} |lm\rangle V_l(r) \langle lm| \tag{9}$$

where $|lm\rangle$ represents the spherical harmonics and $\langle lm|$ is nothing but the projection operator that, when acting on a given function, selects only the angular coordinates. The non-local operator of equation (9) can be decomposed into a sum of different operators where each has a particular symmetry:

$$V_{\mathrm{NL}} = V_{\mathrm{s}} + V_{\mathrm{p}} + V_{\mathrm{d}} + \cdots. \tag{10}$$

For example, the operator V_s acts only on orbitals possessing an s symmetry. From this it is now clear that a different local potential $V_l(r)$ is needed for different l values.

Introducing the closure relation into equation (8) we can write the propagator as

$$K(r_{n+1}, r_n, \tau) = \int \mathrm{d}r\, \langle r_n|\mathrm{e}^{-\epsilon V_{\mathrm{loc}}}|r\rangle \int \mathrm{d}r'\, \langle r|\mathrm{e}^{-\epsilon V_{\mathrm{NL}}}|r'\rangle\langle r'|\mathrm{e}^{-\epsilon T_{\mathrm{op}}}|r_{n+1}\rangle. \tag{11}$$

One can then rewrite the propagator in the following manner:

$$K(r_{n+1}, r_n, \tau) = \int \mathrm{d}r\, \delta(r - r_n)\mathrm{e}^{-\epsilon V_{\mathrm{loc}}(r)} \int \mathrm{d}r'\, \langle r|\mathrm{e}^{-\epsilon V_{\mathrm{NL}}}|r'\rangle\langle r'|\mathrm{e}^{-\epsilon T_{\mathrm{op}}}|r_{n+1}\rangle. \tag{12}$$

Note that in this case $V_{\mathrm{loc}}(r)$ is a function of the position vector r. The free particle density matrix, the last term on the right hand side of equation (12), can be evaluated. The propagator K then becomes

$$K(r_{n+1}, r_n, \tau) = \left(\frac{mP}{2\pi\beta\hbar^2}\right)^{3/2} \mathrm{e}^{-(\beta/P)V_{\mathrm{loc}}(r_n)} \int \mathrm{d}r'\, \langle r_n|\mathrm{e}^{-(\beta/P)V_{\mathrm{NL}}}|r'\rangle \mathrm{e}^{-(mP/2\beta\hbar^2)(\Delta r)^2} \tag{13}$$

where Δr is the difference between the two vectors r' and r_{n+1}. In deriving equation (13), the sampling property of the delta function was used. With a series expansion we carry on the task of evaluating the term involving the non-local pseudopotential operator in equation (13).

The following orthonormalization relation in spherical harmonics:

$$\langle r_n|r'\rangle = \frac{\delta(r_n - r')}{r'^2} \sum_{l,m} Y^*_{lm}(\theta_n, \phi_n) Y_{lm}(\theta', \phi') \tag{14}$$

along with the expression for the kernel [23]

$$\langle r_n|V_{\mathrm{NL}}|r'\rangle = \sum_l \sum_m Y^*_{lm}(\theta_n, \phi_n) V_l(r_n, r') Y_{lm}(\theta', \phi') \tag{15}$$

are helpful in evaluating the terms in the series. It is a straightforward task to evaluate the terms involving higher orders of V_{NL}. If P is large, the short-time propagator may be rewritten in the following manner:

$$\begin{aligned} K(r_{n+1}, r_n, \tau) = {} & 4\pi \left(\frac{\beta C}{\pi}\right)^{2/3} \mathrm{e}^{-(\beta/P)V_{\mathrm{loc}}(r_n)} \int r'^2\, \mathrm{d}r' \int \sin\theta'\, \mathrm{d}\theta' \int \mathrm{d}\phi' \\ & \times \sum_{l,m} Y^*_{lm}(\theta_n, \phi_n) Y_{lm}(\theta', \phi') \frac{\delta(r_n - r')}{r'^2} \mathrm{e}^{-(\beta/P)V_l(r')} \left[\frac{\pi}{4\beta C r' r_{n+1}}\right]^{1/2} \\ & \times \sum_{L,M} Y_{LM}(\theta_{n+1}, \phi_{n+1}) Y^*_{LM}(\theta', \phi') I_{l+1/2}(2\beta C r' r_{n+1}) \mathrm{e}^{-\beta C(r'^2 + r^2_{n+1})} \end{aligned} \tag{16}$$

where

$$C = Pm/2\beta^2\hbar^2. \tag{17}$$

Finally, with further manipulation the expression for the propagator takes the form

$$\begin{aligned} K(r_{n+1}, r_n, \tau) = {} & 4\pi \left(\frac{\beta C}{\pi}\right)^{3/2} \left[\frac{\pi}{4\beta C r_n r_{n+1}}\right]^{1/2} \sum_{l,m} Y^*_{lm}(\theta_n, \phi_n) Y_{lm}(\theta_{n+1}, \phi_{n+1}) \\ & \times \mathrm{e}^{-(\beta/P)[V_{\mathrm{loc}}(r_n) + V_l(r_n)]} I_{l+1/2}(2\beta C r_n r_{n+1}) \mathrm{e}^{-\beta C(r_n^2 + r_{n+1}^2)} \end{aligned} \tag{18}$$

where V_{loc} acts locally in radial coordinates.

Using equation (18), along with the identities

$$e^{-\beta C(\Delta r)^2} = e^{-\beta C(r^2+r_{n+1}^2)} e^{2\beta C r' r_{n+1}\cos\alpha} \tag{19}$$

$$e^{\xi\cos\alpha} = \left(\frac{\pi}{2\xi}\right)^{1/2} \sum_{l=0}^{\infty} (2l+1) P_l(\cos\alpha) I_{l+1/2}(\xi) \tag{20}$$

we can write the partition function for our system in a form that conveys an angular momentum dependence

$$Q \approx \left(\frac{\beta C}{\pi}\right)^{3P/2} \int dr_1\, dr_2 \ldots dr_P \prod_{n=1}^{P} \left[e^{-(\beta/P)V_{loc}(r_n)} \times \left\{ \sum_{l=0}^{\infty} (2l+1) P_l(\cos\alpha)\, \mathfrak{I}_{l+1/2}(\chi)\, e^{-(\beta/P)V_l(r_n)} \right\} e^{-\beta C(r_n - r_{n+1})^2} \right] \tag{21}$$

where we have defined what we call in this paper a newly modified Bessel function as

$$\mathfrak{I}_{l+1/2}(\chi) = (\pi/2\chi)^{1/2} e^{-\chi} I_{l+1/2}(\chi) \tag{22}$$

and

$$\chi = 2\beta C r_n r_{n+1}. \tag{23}$$

In equations (20) and (21) $P_l(\cos\alpha)$ is the Legendre polynomial, and α is the angle between the two positions vectors r_n and r_{n+1}.

3. Application and results

3.1. Effective potential

The summation in the propagator expression, equation (18), runs over all the possible values of the angular momentum quantum number. This is inconvenient in a computer simulation and certain modifications must be made in order to overcome this difficulty. Since the system we are studying is a sodium atom, it is clear that the core does not include any angular momentum state higher than one. Thus, for values of l that are larger than one, we approximate the non-local pseudopotential by a local pseudopotential [15, 17, 24]. With this approximation, the propagator of the electron in the field of the sodium ion takes the following form:

$$K_{Na^+} = (\beta C/\pi)^{3/2} e^{-(\beta/P)V_{loc}} e^{-\beta C(r_n - r_{n+1})^2} \{ P_0(\cos\alpha)\, \mathfrak{I}_{1/2}(2\beta C r_n r_{n+1}) [e^{-(\beta/P)V_0(r_n)} - e^{-(\beta/P)V_1(r_n)}] \} + (\beta C/\pi)^{3/2} e^{-(\beta/P)[V_{loc}(r_n)+V_1(r_n)]}\, e^{-\beta C(r_n - r_{n+1})^2} \tag{24}$$

where the zero-order Legendre polynomial $P_0(\cos\alpha) = 1$.

In order to proceed with a molecular dynamics simulation for our quantum system, we need an effective potential to describe the interactions of the nodes (beads) with each other,

and with the sodium ion. It is desirable that the effective potential be defined by writing the partition function in a classical form

$$Q \approx \left(\frac{\beta C}{\pi}\right)^{3P/2} \int \left[\prod_{n=1}^{P} \mathrm{d}r_n\right] \mathrm{e}^{-\beta V_{\mathrm{eff}}(r_1,\ldots,r_P)}. \tag{25}$$

However, the partition function for our system cannot be put in this form without some approximations. This is because the propagator in equation (24) involves positive and negative terms.

For the case of Na^+ we define an approximate partition function in the following manner:

$$Q_{\mathrm{Na}^+} \approx \left(\frac{\beta C}{\pi}\right)^{3P/2} \int' \mathrm{d}r \ldots \mathrm{d}r_P \exp\left\{\sum_{n=1}^{P} \ln[\![\mathrm{e}^{-(\beta/P)V_{\mathrm{loc}}} \mathrm{e}^{-\beta C(r_n - r_{n+1})^2} \Im_{1/2}(2\beta C r_n r_{n+1}) \times [\mathrm{e}^{-(\beta/P)V_0(r_n)} - \mathrm{e}^{-(\beta/P)V_1(r_n)}] + \mathrm{e}^{-(\beta/P)[V_{\mathrm{loc}}+V_1(r_n)]} \mathrm{e}^{-\beta C(r_n - r_{n+1})^2}]\!]\right\} \tag{26}$$

where the symbols [[ ]] are merely delimiters and carry no physical meaning, and the prime sign over the integral limits it to states that give a positive value for the argument of the natural logarithmic function in the integrand. We arrive at equation (26) by neglecting the contribution of the states that give a negative value of the propagator in equation (24). These negative values will arise for configurations of states, n and $n+1$, such that $\pi/2 \leqslant \alpha \leqslant \pi$. These configurations appear mainly near the core since large P (short-time approximation for the path PI) leads to short distances between consecutive nodes. Therefore, away from the core we expect our approximation of the partition function to give more accurate results than when the electron is in the core. This is because the angle subtended by two consecutive nodes decreases as the nodes move away from the core region. It is only when the nodes approach the center of the core that some of the angles fall in the range mentioned above, and thus giving us negative propagators.

Upon inspecting the partition function we can see that the approximate effective potential is readily obtained as

$$V_{\mathrm{eff}} = -\frac{1}{\beta} \sum_{n=1}^{P} \ln\{\mathrm{e}^{-(\beta/P)V_{\mathrm{loc}}} \mathrm{e}^{-\beta C(r_n - r_{n+1})^2} \Im_{1/2}(2\beta C r_n r_{n+1}) \times [\mathrm{e}^{-(\beta/P)V_0(r_n)} - \mathrm{e}^{-(\beta/P)V_1(r_n)}] + \mathrm{e}^{-(\beta/P)[V_{\mathrm{loc}}+V_1(r_n)]} \mathrm{e}^{-\beta C(r_n - r_{n+1})^2}\}. \tag{27}$$

This potential could be easily rewritten in the following fashion:

$$V_{\mathrm{eff}} = \sum_{n=1}^{P} C(r_n - r_{n+1})^2 + \frac{V_1(r_n) + V_{\mathrm{loc}}}{P} - \frac{1}{\beta} \ln\{1 + \Im_{1/2}(2\beta C r_n r_{n+1})\, \mathrm{e}^{2\beta C r_n r_{n+1}(1-\cos\alpha)} [\mathrm{e}^{-(\beta/P)(V_0 - V_1)} - 1]\}. \tag{28}$$

Although approximate, equation (28) conveys a plausible physical picture. The first term represents the harmonic potential due to the springs linking neighboring nodes. The second term represents the external potential felt by each node. The inverse temperature β is a large positive number. The number of nodes P is also large, which in turn makes the

angle between the position vectors of two neighboring nodes extremely small. The newly modified Bessel function $\Im(2\beta C r_n r_{n+1})$ is always positive and has a maximum value of one as shown in figure 1. Thus, the third term gives rise to a centrifugal effect (a positive quantity) that is needed to keep the valence electron from collapsing into the core region. One can then draw the analogy between this effective potential and the components of the regular radial effective potential that is encountered in the radial part of the Schrödinger equation. Note that this effective potential offers an infinite energy barrier, which guarantees that states with negative $[\![\,]\!]$ will never occur in our calculations.

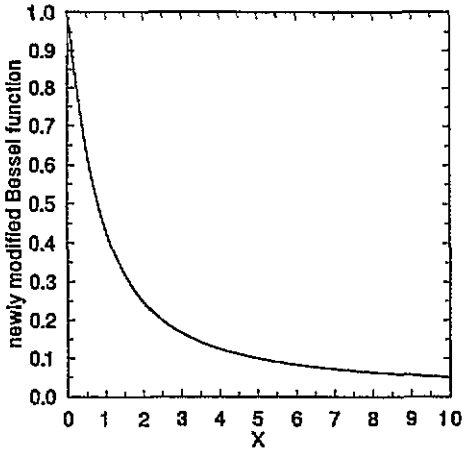

Figure 1. A plot of the newly modified Bessel function.

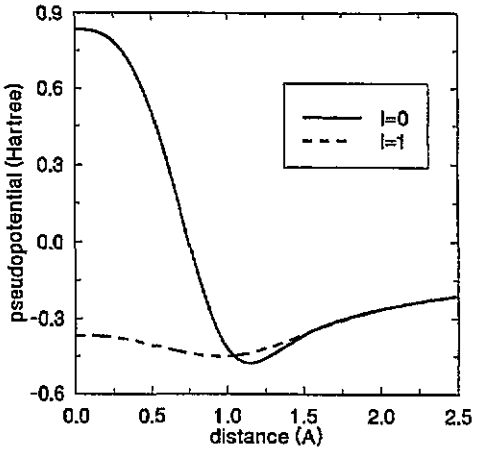

Figure 2. Non-local pseudopotentials for Na that were generated using the BHS method [17].

3.2. Simulation

The molecular dynamics simulations were conducted at a constant temperature of 1000 K. This temperature is kept constant throughout the simulation by using a momentum rescaling thermostat [25]. The total effective force on the electron is the vector sum of all the forces acting on the nodes. For the nth node we write

$$F_n = -\partial V_{\text{eff}}/\partial r_n. \tag{29}$$

The equations of motion were solved using the leapfrog algorithm with time integration step $\Delta t = 1.3 \times 10^{-17}$ s. The electron was represented by a chain consisting of a set of P nodes (beads). Each node has an arbitrary mass of 1 au. The simulation was conducted twice for each state. In one simulation the electron was represented by 384 nodes, while in the other 490 nodes were used. This high number of nodes is needed because of the steep repulsive potential that exists in the core region. Although these numbers could be over cautious, a large number of nodes is still needed in our case since we are using the Trotter expansion without higher-order correction terms. Using this version of the Trotter formula, Li and Broughton noted the need for 100–150 nodes to simulate an electron in the potential field of a lithium ion at approximately 1000 K [26]. Each simulation run was carried on for 400 000 time steps.

In figure 2 we show the pseudopotential for $l = 0$ and $l = 1$ in sodium. These pseudopotentials are non-singular with their derivation based on a first-principles approach

by BHS [16]. One can readily see the steep repulsive barrier in the core region for the pseudopotential that corresponds to $l = 0$. By contrast, the pseudopotential for $l = 1$ does not show such a steepness in the core region. In the absence of a centrifugal barrier, the 3p electron would collapse into the core region.

3.3. Results

There are two approaches to simulate the electron in the 3s state. The first approach relies on sampling the states using the effective potential exactly as it appears in equation (28). This means that the pseudopotentials used are those that appear in figure 2, with no alteration or modification to their values at any position of the quantum particle. This is very important if we are to study molecular systems where the full non-locality is vital. However due to the attractive nature of the 3p pseudopotential in the core region, the 3s electron will be pulled towards the core. At 1000 K with $P = 384$ and 490 the approximate distances between two subsequent nodes are 0.84 Å and 0.74 Å respectively. These distances are comparable to the core size itself. This means that as the electron approaches the core, we expect to have more negative propagators. Neglecting the increasing number of these states, as the electron moves deeper into the core, will weaken the accuracy of the centrifugal effect in our effective potential. In this case, the amplitude of the electron will be shifted towards the core as shown in figure 3. In this case, our results agree qualitatively with the 3s amplitude constructed by Melius and Goddard [17] (dashed line), who used the CHF method.

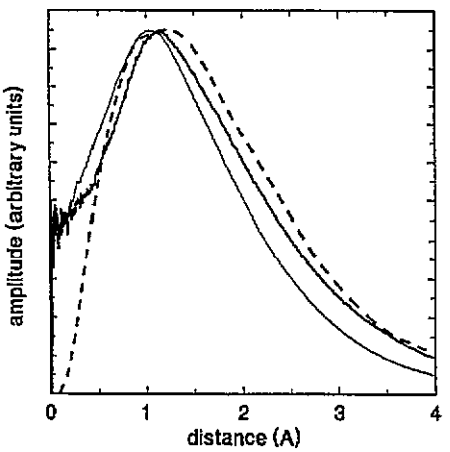

Figure 3. The pseudoamplitude for the 3s state in Na. This work is shown in solid line: fine line, the non-local case; heavy line, the local case. Dashed line, Melius and Goddard. The number of nodes is 384.

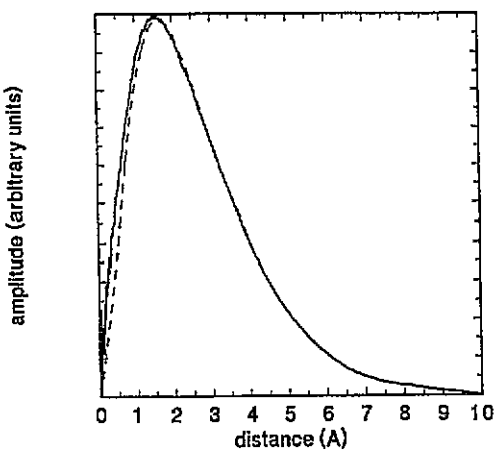

Figure 4. The 3p amplitude in our case (solid line) and that of Melius and Goddard (dashed line). The number of nodes is 384.

In order to overcome the above mentioned problem, a second approach can be taken to avoid the attractive effects of V_1 on the 3s electron. In this case, we need to make certain that the electron feels only the effects of the 3s pseudopotential. This may be achieved by setting $V_1 = V_0$ in the propagator equation. The results of the simulation for this 3s state is also shown in figure 3. As depicted in the figure, the position of the peak and the tail region of our results agree reasonably well with the CHF amplitude.

In either approach, the resulting amplitudes for the 384- and the 490-node systems came to an exact agreement with each other. This suggests that 384 nodes is a satisfactory upper limit for P. The amplitudes shown in figure 3 are for the 384-node system.

The noise that appears deep in the core is not inherent to our formulation. Indeed the electron density calculated in our simulation vanishes near the origin. The amplitude is found by taking the square root of the electron density and then dividing the result by r. This division becomes very noisy as r approaches zero.

For the 3p state, the existence of a core orbital of the same symmetry will have a dragging effect on the 3p electron and the electron will eventually be sucked into the core. The BHS pseudopotential does not have in this region a sufficient repulsive force, as seen in figure 2. In order to avoid this problem, we loaded our effective potential with an artificial potential barrier that prevented the electron from moving into the more energetically favorable 3s state. This is accomplished by setting $V_0(r)$ in the effective potential to a constant value for all r and equal to the maximum difference between the 3p and 3s pseudopotentials in the core region. This energy barrier is sufficient to keep the electron from behaving like a 3s state, and from wandering in the core region. This will limit the occurrence of the negative propagator states, and thus our approximate partition function should give the required results. Figure 4 depicts the 3p orbit for 384 nodes. As shown in this figure, the 3p amplitude obtained with our formulation agrees very favorably with that of the CHF method (dashed line). 384 is a sufficient number of nodes to simulate the electron in this excited state. To demonstrate this, we superimpose in figure 5 the amplitude of the 3p state using 490 nodes for the electron over that of figure 4. The result, seen in figure 5, shows basically no difference between the two amplitudes.

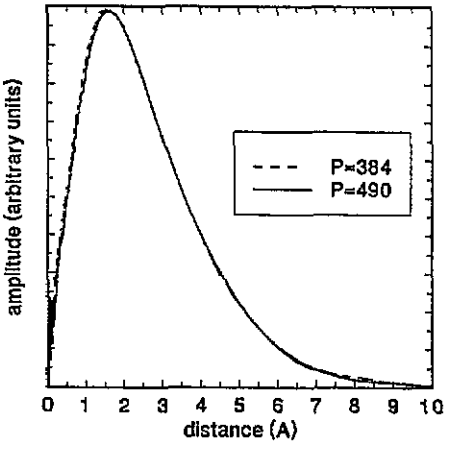

Figure 5. The 3p amplitude in the case of 490 nodes superimposed over the results shown in figure 4.

The reader should be reminded that we do not anticipate the amplitudes in our case to come to a good accord, everywhere in space, with those calculated using CHF. This is because of the basic difference between the two approaches. The effective potentials used by Melius and Goddard were derived from CHF orbitals, whereas the BHS pseudopotentials that we use in this paper were obtained based on an all-electron calculation using the local density approximation for the exchange and correlation potential. However, outside the core region the amplitudes obtained using the CHF method coincide accurately with those of

Hartree–Fock and minimum-kinetic-energy methods [17]. In this region electronic amplitude is anticipated to be method independent, thus allowing us to make a valid comparison.

After the system reached equilibrium we took some snapshots of the configurational distribution of the nodes. These shots were then projected onto two dimensions to help give a qualitative picture of the electronic distribution in the particular orbital state. The spherical symmetry characteristic of the s state is obvious in figure 6. It is further interesting to note how the nodes are populated away from the origin in figure 7, which is characteristic of the p orbital.

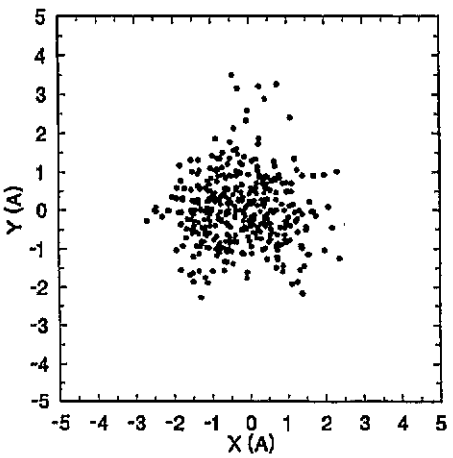

Figure 6. A projected snapshot of the configurational distribution of the 3s electron. The number of nodes in this case is 384. The nucleus is at the origin.

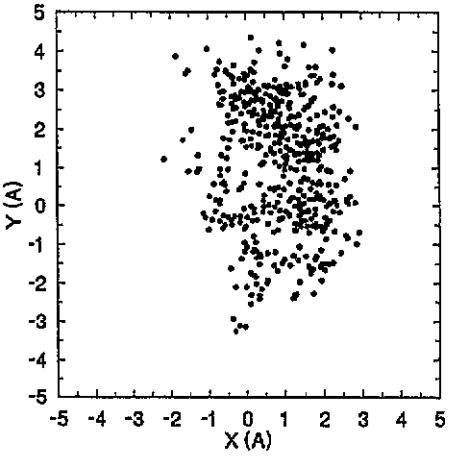

Figure 7. A projected snapshot of the configurational distribution of the electron in a 3p state. The number of nodes in this case is 490. The nucleus is at the origin.

4. Conclusion

In order to be able to perform PIMD of a molecular system, one needs to incorporate non-locality in the PI. In this paper, we have illustrated a method for the incorporation of non-local pseudopotentials into the PI using polar coordinates. An approximate effective potential deduced from the derivation was implemented in an open boundary molecular dynamics simulation. The system simulated was a single valence electron of sodium in its 3s and 3p states. The electronic 3s amplitude calculated using our formulation is in qualitative agreement with amplitudes obtained through other methods such as the CHF method. In order to keep full non-local effects, which is very important in molecular systems, and improve the accuracy of the method a corrective factor may be incorporated into our effective potential to account for the neglect of the negative propagator states in the core region. This aspect will be the subject of a future work.

The simplicity and ease of numerically implementing our formulation makes it attractive in the case of atoms or ions with a single valence electron and a maximum angular momentum state $l = 1$ in the core. For elements that fall into this category, different pseudopotentials must be incorporated into our equations. Such pseudopotential data are tabulated by BHS [16]. The extension of our method to incorporate d states is straightforward, but requires some bookkeeping. This extension is currently under investigation. We are

working on calculating the 3s and 3p energies to compare them with those obtained using other techniques. Also, we are using our derivation to study the behavior of an electron in the field of a lithium ion. The initial results are very encouraging.

For systems with more than one valence electron, with a maximum of $l = 1$ in the core, our derivation obviously does not hold. This is because of the indistinguishability that must be incorporated into the PI. Problems arising from the Fermi statistics are anticipated here due to the negative terms that are carried in the partition function. One way to overcome this difficulty is to use the Hall approximation method of dealing with exchange in the PI [10].

Acknowledgment

We would like to thank Mr Jonathan D Weinberg for his critical reading of this manuscript.

References

[1] Chandler D and Wolynes P 1981 *J. Chem. Phys.* 74 4078
[2] Parrinello M and Rahman A 1984 *J. Chem. Phys.* **80** 860
[3] Sprik M, Klein R M L and Chandler D 1985 *Phys. Rev.* B **32** 545
[4] Sprik M, Impey R W and Klein M L 1986 *Phys. Rev. Lett.* **56** 2326
[5] Broughton J and Abraham F 1988 *J. Phys. Chem.* **92** 3274
[6] Ceperley D M and Pollock E L 1986 *Phys. Rev. Lett.* **56** 474
[7] Gillan M J 1987 *Phys. Rev. Lett.* **58** 563; 1988 *Phil. Mag.* A **58** 257
[8] Hall R W 1989 *Chem. Phys. Lett.* **160** 520
[9] Lyubartsev A P and Vorontsov-Velyaminov P N 1993 *Phys. Rev.* A **48** 4075
[10] Hall R W 1988 *J. Chem. Phys.* **89** 4212
[11] Iyer V, Jabbour G E, Deymier P A and Lee C Y 1993 *Modelling Simul. Mater. Sci. Eng.* **1** 361
[12] Chakravarty C 1993 *J. Chem. Phys.* **99** 8038
[13] Fahy S, Wang X W and Louie S G 1990 *Phys. Rev.* B **42** 3503
[14] Mitáš L, Shirley E and Ceperly D 1991 *J. Chem. Phys.* **95** 3467
[15] Galli G and Parrinello M 1991 *Computer Simulation in Materials Science (NATO ASI Series E: Applied Sciences 205)* ed M Meyer and V Pontikis (Dordrecht: Kluwer)
[16] Bachelet G B, Hamann D R and Schlüter M 1982 *Phys. Rev.* B **26** 4199
[17] Melius C F and Goddard W A III 1974 *Phys. Rev.* A **10** 1528
[18] Kleinert H 1990 *Path Integrals in Quantum Mechanics, Statistics, and Polymer Physics* (Singapore: World Scientific)
[19] Edwards S F and Gulyaev Y V 1964 *Proc. R. Soc.* A **279** 229
[20] Peak D and Inomata A 1969 *J. Math. Phys.* **10** 1422
[21] Cohen M and Heine V 1961 *Phys. Rev.* **122** 1821
[22] Abrenkov I V and Heine V 1965 *Phil. Mag.* **12** 529
[23] Gonze X, Stumpf R and Scheffler M 1991 *Phys. Rev.* B **44** 8503
[24] Szasz L 1985 *Pseudopotential Theory of Atoms and Molecules* (New York: Wiley)
[25] Woodcock L V 1971 *Chem. Phys. Lett.* **10** 257
[26] Li X P and Broughton J Q 1987 *J. Chem. Phys.* **86** 5094